

Ion implantation of CdTe single crystals

Tomasz Wiecek¹, Volodymir Popovich², Mariusz Bester³, Marian Kuzma³

¹Physics Chair, Rzeszow University of Technology, al. Powstańców Warszawy 12, 35-959 Rzeszow, Poland

²Department of Fundamental Technologies, Ivan Franko Drogobych State Pedagogical University, Ivan Franko 24, 82100 Drogobych, Ukraine

³Biophysics Chair, Rzeszow University, S. Pigionia 1, 35-959 Rzeszow, Poland

Abstract. Ion implantation is a technique which is widely used in industry for unique modification of metal surface for medical applications. In semiconductor silicon technology ion implantation is also widely used for thin layer electronic or optoelectronic devices production. For other semiconductor materials this technique is still at an early stage. In this paper based on literature data we present the main features of the implantation of CdTe single crystals as well as some of the major problems which are likely to occur when dealing with them. The most unexpected feature is the high resistance of these crystals against the amorphization caused by ion implantation even at high doses (10^{17} 1/cm²). The second property is the disposal of defects much deeper in the sample than it follows from the modeling calculations. The outline of principles of the ion implantation is included in the paper. The data based on RBS measurements and modeling results obtained by using SRIM software were taken into account.

1 Introduction

Doping of single crystals of CdTe is a troublesome task in AIBVI devices technology due to the segregation effects, the presence of compensating defects in the crystal and due to disturbing of stoichiometry [1]. There are three main methods of doping of CdTe crystals: the first being the addition of species during growth, the second one reckoning on the diffusion of dopants using annealing, and the third one which is the ion implantation. The two first methods are extensively experimentally investigated for wide amount of dopant elements (see Chapter B5 in [1]). Contrarily, the ion implantation has been studied for two dopants only: As and Bi. The aim of such studies was type conversion for p-n junction formation. Ion implantation is broadly applied in semiconductor, and metallurgy technology [2,3] because of its advantage such as the low temperature process which allows to apply polymer masks in photolithography. Implantation is a kind of technology which allows introducing non-soluble elements into the material [4]. The process of irradiation is uniform in surface. It is easy to control the concentration of dopants introduced into depth. Thanks to the use of masks of various width, the concentration of dopants may be changed in various areas of surface in one cycle of implantation. The implantation process is well modeled with Monte-Carlo simulation. Popular software for such modeling is SRIM code [5]. The experimental results agree very well with model results for Si, AIII-BV semiconductors as well as for metals. However, the parameters of implanted CdTe crystals differ considerably from those pointed by SRIM

simulation. Therefore, the implantation of CdTe is less applicable in microelectronic technology of devices based on CdTe material. In this paper we present the problems encountered with ion implantation of CdTe. In Section 2 we present preparation of samples for implantation. The physical principles of implantation are discussed in Section 3. The post implanted annealing of the samples is analysed in this section as well. In Section 4 the classical problems with implantation of B and As into CdTe in the aim of p-n junction formation are outlined. Structure damage of the samples after implantation is addressed in Section 5 basing mainly on the excellent paper of Rischau et al. [6].

Affiliations of authors should be typed in 9-point Times. They should be preceded by a numerical superscript corresponding to the same superscript after the name of the author concerned. Please ensure that affiliations are as full and complete as possible and include the country.

2 Preimplantation sample preparation

The majority of the samples were prepared in the form of platelets of a size of 5x4x1 mm³. Platelets were mechanically polished and chemically etched with a solution of bromine in methanol. The preimplantation annealing of Te rich CdTe in Cd vapour was used for 36 h at 500°C ensuring Cd overpressure of 0.5 Torr [7].

The implantation with As⁺ at room temperature is not efficient while the damage of structure is so great that the sample becomes semi insulating. The recovery of crystal structure of the crystal structure was not achieved by post implanted annealing within two days at 650°C

[8]. Therefore, the hot temperature implantation had to be applied. For this, the obstacle of high vapour pressure of CdTe should be removed by encapsulating of the samples. It was done by means of SiO₂ layers. The layers with 150 nm are proper for As⁺ ions implantation. SiO₂ encapsulating layers are stable for temperatures not exceeding 525° C [8].

3 Implantation overview, implantation parameters and instrumentation

The main implantation parameters are: temperature of target (T), energy of ions (E), ion current density (I), time of implantation (t), total dose (TD).

The typical set up for ion implantation consists of (Fig.1) source of ions, magnet for ion selection, accelerator, scanning electrostatic plates, beam diaphragm, The environment for all these parts/ factors is high vacuum (10⁻⁷ Torr).

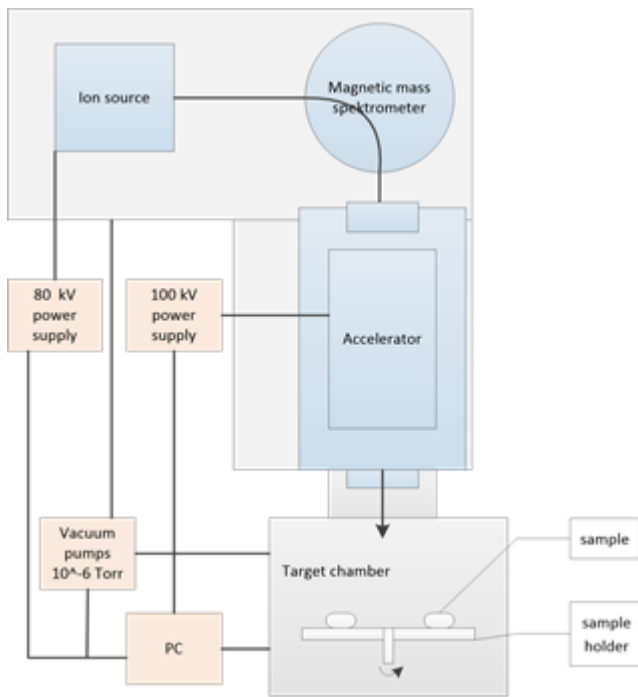


Fig. 1. Scheme of set up for ion implantation.

Ion current density is measured using Faraday box as:

$$j = I / q e A, \quad (1)$$

where A is the area of Faraday box, q is the ionicity number of ions (usually $q = 1$), e is the elementary charge. The typical currents in ion implantation are 1 μ A – 10 mA.

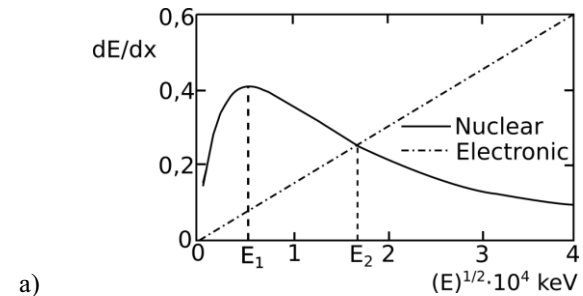
The fluency (dose) is defined as

$$\Phi = j \cdot t, \quad (2)$$

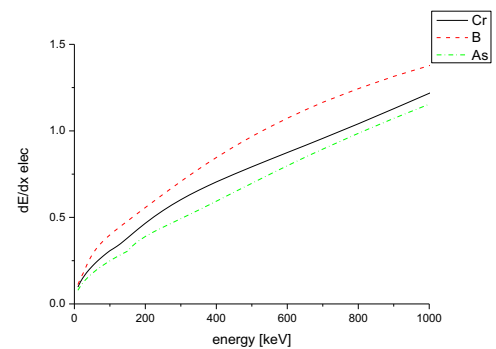
where t is the implantation time.

A dose gives a number of ions per unit area in whole depths of samples. It is not with simple relation to concentration of dopants (the number of atoms per unit volume while the concentration depends strongly on the depth although laterally it is constant).

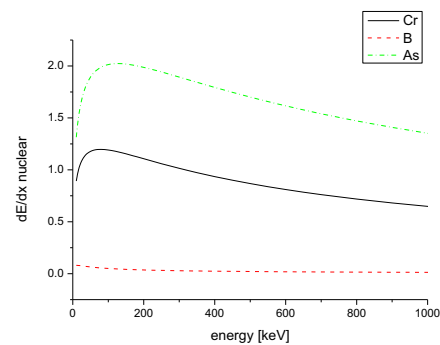
Ions with high energy (usually 50 – 750keV) penetrates the near surface layer (up to 1 μ m for high energy). The ions undergo collisions with nucleons or electron of atoms of the target. These collisions are cascade and ions gradually lose the energy. Rate of energy loss into depth dE/dx depends on energy of ions and material. The dependence of the rate of energy loss for collision with electrons increases linearly versus $E^{1/2}$. Contrary to this, such dependence for collisions with nucleons is nonlinear showing clear maximum at energy in small range of energy E as it is seen in Fig. 2a. In this range of energy the nuclear loss of energy is dominated whereas for high energy ions the electronic loss is prevailing. In Fig. 2a and 2b Such rate of energy loss for CdTe crystals implanted with Cr, B, and As were calculated using SRIM code [5] and the results are demonstrated in Fig.2b and Fig.2c.



a)



b)



c)

Fig. 2. Dependence of the rate of energy loss on $E^{1/2}$ (a), electronic (b) and nuclear (c) rate of energy loss for CdTe implanted with Cr,B and As (results of SRIM simulations).

Irradiation of a solid with high energy ions leads to numerous crystal defect formations on the surface as well in the near surface layer [9-12] :

1) surface defects are: sputtering , roughening, swelling, surface nanopatterning (see[13] and ref. therein),

2) in the bulk the following defects are created: vacancies, interstitials, pattern formation ,void formation, recombination, diffusion, sponge structure formation.

In the aim to remove these defects or part of them the annealing after implantation is applied. However, the annealing may create new defects like nucleation of existing defects, nanocluster formation, voids formation (by nucleation of vacancies) etc. [14-16].

The implantation of a small area on the surface of the target results in formation of bulk distribution of dopants in x,y, z space in the form of a ball (Fig .3a).

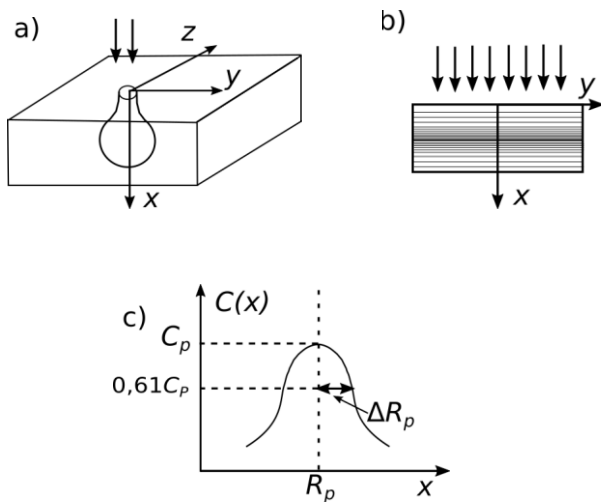


Fig. 3. Scheme of concentration distribution of defects (or dopants) in the sample implanted by stable ion beam (a), implanted by scanning ion beam (b), one-dimensional Gaussian approximation of defects distribution (c).

Usually the target is scanned by ion-beam , therefore the superposition of implantation at all the lateral position on a surface results in one-dimensional depth profile of dopant (Fig . 3b). Such profile can be approximated by Gaussian function (Fig. 3c):

$$C(x) = C_p \exp [- (x- R_p)^2 / 2(\Delta R_p)^2], \quad (3)$$

where R_p is a projected range, and ΔR_p is a longitudinal straggle.

The parameters R_p and ΔR_p depend in a near linear way on graphs $\log R_p$ versus $\log E$ or $\log \Delta R_p$ versus $\log E$ almost for all the elements implanted.

There are two aims of the post implanted annealing:

- 1) Restoring the crystallinity of the sample,
 - 2) Introducing dopants into substitute sites of the crystal lattice in order to activate them(electrically or optically).
- Three types of post implanted annealing are applied:
- 1) Steady annealing (e. g. $T = 650^\circ\text{C}$, in time 1 hour for CdTe).
 - 2) Rapid thermal annealing [17] using the xenon lamps (heating up to 1000°C with velocity more then 50°C/s).

3) Pulsed laser annealing with nanosecond length of pulses (see [18] and ref. therein).

4 The p-n junction formation in CdTe crystals

In the paper of Donnelly at al. [8] the following parameters were established with the aim of formation of type conversion of n - CdTe into p-CdTe by As^+ implantation : $T = 500^\circ\text{C}$, $E = 400 \text{ keV}$, $I = 0.5 \mu\text{A}/\text{cm}^2$, $t = 15 \text{ min}$, dose = $3 \cdot 10^{15}/\text{cm}^2$. The p-n junction formation was supported by U-I characteristics which show forward resistance of 30Ω and reverse breakdown of 40V .

Chu [7] implanted n-type undoped CdTe by As^+ ions with energy 60 keV , and dose 10^{15} . Electrical and photovoltaic properties were measured. Density of holes as a function of distance from implanted surface were determined by Hall measurements after periodic successive etching of the sample. From these measurements it follows that the effects of the implantation were observed at depths greater then 250 nm , whereas the modeling projected range for As^+ ions at such energy is about $29 \pm 17 \text{ nm}$.

Further continuation of implantation of CdTe crystals in order to obtain p- n⁺ junction was ensured for p-type $\text{Cd}_x\text{Hg}_{1-x}\text{Te}$ [19,20]. The n- type conductivity may be produced by implantation of B [21], Al [22], In [23], Zn [23], Hg [24] as well as Au and P (see Capper [1] p.160). The electrical properties of ion implanted layers in $\text{Cd}_x\text{Hg}_{1-x}\text{Te}$ were investigated by Margalit et al. [20]. Dopants (B, Ar, In, P, Au) were implanted at 150 keV , with dose $10^{11} - 10^{15} \text{ 1/cm}^2$. The samples were annealed at temperature 150°C during 24 h in vacuum The samples were encapsulated by 200 nm thick CdTe layer. The results demonstrate that the crystal structure damage rather than kind of dopants converts p-type into n-type conductivity. The authors proposed to apply the implantation for formation of accumulated surface for surface passivation and for formation of Ohmic contacts on n-type material.

Recently, ion implantation of CdHgTe is well known method for fabrication infrared photovoltaic devices. The paper [25] presents a short review on technology of production of CdHgTe fotodiodes by implantation As into n-type matrix.

5 Ion – beam induced damage in CdTe

Implantation damage in CdTe implanted with isotope of host ions ^{111}Cd at 60 keV at room temperature were investigated by Achtziger et al. [26]. Dose was low: $2 \cdot 10^{11} \text{ 1/cm}^2 - 6 \cdot 10^{11} \text{ 1/cm}^2$ The host atoms were chosen for implantation in the aim to avoid any chemical activity of implants. Annealing treatment was carried out for several temperatures in the range $723\text{K}-1073\text{K}$ Characterization of the implanted and annealed samples was made by perturbed angular spectroscopy and by deep-level transient spectroscopy . For this last technique parallelly, the set of nonimplanted samples was annealed and measured providing good reference data. The

conclusions from these studies are: 1) At low doses all implanted atoms occupy substitutional lattice sites. Local crystal environment of these atoms is almost perfect before annealing; after annealing at 673K it is perfect, 2) After implantation no additional electrically active centers have been observed.

C. W. Rischau et al. [6] have implanted CdTe single crystals with orientation (111) and (112). As dopants two types of ions were chosen: the light ions Ar^+ and the heavy ions Sb^{++} having mass comparable with masses of self Cd and Te atoms. The implantation was carried out in two temperatures: 5 K and in room temperature. These two implantation temperatures should help to decide which mechanism of implanted defects formation, thermal or non-thermal is responsible for an unusually small, but deep damage of structure in CdTe. The energy of ions was 270 keV for Ar^+ and 730 keV for Sb^{++} . Such values of energy were chosen to obtain the projected range for both ions $R_p = 220$ nm. Such value lies well beyond of the positions of surface atoms Cd and Te in RBS spectra. The dose was ranging from 10^{11} $1/\text{cm}^2$ to 10^{17} $1/\text{cm}^2$. The RBS spectra of samples irradiated with Ar^+ ions did not differ considerably for both orientations of samples at room temperature. Moreover, at low temperature (15 K) this spectra are similar to those in room temperature. There is expressive dependence of lattice disorder on the dose. In spite of this, the channeling spectra do not reach random spectrum even for the highest dose $5 \cdot 10^{16}$ $1/\text{cm}^2$. This indicates that the crystal structure is resistive against amorphization even at a dose of 10^{17} $1/\text{cm}^2$. The defect distribution obtained from RBS spectra show deformed Gaussian profiles with $R_p = 250$ nm independently on the orientation of crystals at room temperature. The tail of distribution is long and is equal to $z = 2R_p$ up to $z = 4R_p$. This is a great discrepancy with SRIM results. The defects distribution at 15 K differs considerably from these latter. At doses higher than $2 \cdot 10^{15}$ the distribution is flat extended up to $4 R_p$ with the maximum at 350 nm independent on the orientation and type of ions. There is also significant increase of defects at surface of the sample. This surface damage increases significantly with the dose increase. However, for both temperatures the buried damage layer placed in the dept 100 nm below the surface and having the width of about 500 nm is formed, but this layer is not amorphous. Taking these results into consideration, Rischau [6] concluded that the high resistance of the CdTe crystals to amorphization follows not from thermal effects but from high ionicity of the crystal studied. Such conclusion were formulated earlier by Gettings at al. [27] and by Uzan-Saguy et al.[28].

Ion implantation of heavy Xe ions into (111) oriented single crystals of CdTe was studied by Petric at al. in the paper [29]. The disorder was investigated using Rutherford backscattering spectrometry (RBS) with He^+ ions [30]. The simulation was done using the SRIM software [5]. The energy of ions was 350 keV and the doses were as follows: $1 \cdot 10^{13} 1/\text{cm}^2$, $2 \cdot 10^{13} 1/\text{cm}^2$, $3 \cdot 10^{13} 1/\text{cm}^2$, $4 \cdot 10^{13} 1/\text{cm}^2$, $6 \cdot 10^{13} 1/\text{cm}^2$, $8 \cdot 10^{13} 1/\text{cm}^2$, $12 \cdot 10^{13} 1/\text{cm}^2$, $16 \cdot 10^{13} 1/\text{cm}^2$. Parallely, for comparison, an identical implantation was done on Si single crystals. The experimental results from RBS measurements and

results from modeling (SRIM) exhibit a great difference in full width at half maximum (FWHM) of damage profile created by Xe ions. For Si samples the FWHM is 150 nm whereas for CdTe samples the FWHM is 90 nm. These values are confirmed by RBS analysis. Moreover, RBS spectra made for Si and CdTe, both implanted with the Xe ions, show the great influence of disorder on the dose in the case of Si sample. For dose $6 \cdot 10^{14} 1/\text{cm}^2$ the channeling spectrum is comparable with the spectrum of random RBS. Contrary to this, in the case of CdTe the channeling spectra for all doses lie near the virgin spectrum which means that the disorder is very weak even for doses exceeding amorphization threshold calculated from the SRIM code (several 10^{16} $1/\text{cm}^2$). From the tails of RBS spectra follows that the extended defects, mainly dislocation loops, prevail in this material after implantation. This seems to be in conformity with results presented in papers of Leo et al. [31-33] where the formation of dislocation loops was explained by high mobility of interstitial Te and enhanced recombination of defects in the depth of the sample. On the other hand, the defects near the surface were grasped by the surface and therefore the near surface layer was protected again amorphization even for high doses.

6 CONCLUSIONS

Usually, the samples are encapsulated before implantation. It seems that this rule should be obligatory in the case of CdTe implantation with high energy. However, this problem is omitted in the works cited. The high stability of the crystal structure seems to promise auspicious future of this material. Its application in doping of new elements allows to obtain new properties of this material. Heavy doping with magnetic ions seems to be one of these prospective new application of ion implantation of CdTe crystals or layers.

Acknowledgments

The support from the Center for Innovation and Transfer of Natural Science and Engineering Knowledge at the University of Rzeszow is gratefully acknowledged.

References

1. P. Capper, *Properties of Narrow-Gap Cadmium-Based Compounds*, (United Kingdom 1994)
2. J. F. Ziegler (ed.) *Ion Implantation (Science and Technology*, Academic Press 1988)
3. E. Rimini, *Ion Implantation, Basic to Device Fabrication*, (Kluwer Academic Publ., Boston 1995)
4. O. Meyer, A. Tuross, *Materials Science Reports* **2**, 7, 373-468 (1987)
5. The Stopping and Range of Ions in Matter, <http://www.srim.org>.
6. C.W. Rischau, C.S. Schnohr, E. Wendler, W. Wesch, *J. Appl. Phys.* **109**, 113531 (2011)

7. M. Chu, A.L. Fahrenbruch, R.H. Bube, J.F. Gibbons, *J. Appl. Phys.* **49**, 322 (1978)
8. J.P. Donnelly, A.G. Foyt, E.D. Hinkley, W.T. Lindley, J.O. Dimmock, *Appl. Phys. Lett.* **12**, 303 (1968)
9. R. Böttger, K.H. Heinig, L. Bischoff, B. Liedke, R. Hübner, W. Pilz, *Phys. Status Solidi - Rapid Res. Lett.* **7**, 501 (2013)
10. R.A. Wilhelm, E. Gruber, R. Ritter, R. Heller, S. Facsko, F. Aumayr, *Phys. Rev. Lett.* **112**, 153201 (2014)
11. R. Böttger, K.H. Heinig, L. Bischoff, B. Liedke, S. Facsko, *Appl. Phys. A Mater. Sci. Process.* **113**, 59 (2013)
12. R. Ritter, R.A. Wilhelm, M. Stöger-Pollach, R. Heller, A. Mücklich, U. Werner, et al., *Appl. Phys. Lett.* **102**, 063112 (2013)
13. O. El-Atwani, S.A. Norris, K. Ludwig, S. Gonderman, J.P. Allain, *Sci. Rep.* **5**, 18207 (2015) 18207
14. S. Zhou, K. Potzger, G. Zhang, A. Mücklich, F. Eichhorn, N. Schell, et al., *Phys. Rev. B* **75**, 085203 (2007)
15. S. Zhou, K. Potzger, J. Von Borany, R. Grötzschel, W. Skorupa, M. Helm, et al., *Phys. Rev. B* **77**, 035209 (2008)
16. S. Zhou, A. Shalimov, K. Potzger, N.M. Jeutter, C. Baetz, M. Helm, et al., *Appl. Phys. Lett.* **95**, 192505 (2009)
17. T.E. Seidel, D.J. Lischner, C.S. Pai, R.V. Knoell, D.M. Maher, D.C. Jacobson, *Nuclear Instruments and Methods in Physics Research Section B: Beam Interactions with Materials and Atoms*, 7–8, Part 1, 251-260 (1985)
18. S. Zhou, Dilute ferromagnetic semiconductors prepared by the combination of ion implantation with pulse laser melting (Topic Review), *J. Phys. D: Appl. Phys.* **48**, 263001 (2015).
19. C. Uzan-Saguy, *J. Vac. Sci. Technol. A Vacuum, Surfaces, Film.* **10**, 3246 (1992)
20. S. Margalit, Y. Nemirovsky, I. Rotstein, *J. Appl. Phys.* **50**, 6386 (1979)
21. M. Lanir, A.H.B. Vanderwyck, and C.C. Wang, *J. Appl. Phys.* **49**, 6182 (1978)
22. J. Marine and C. Motte, *Appl. Phys. Lett.* **23**, 450 (1973)
23. E. Igras, J. Piotrowski, and I.Z. Higersberger, *Electron Technol.* **10**, 63 (1977)
24. G. Fiorito, G. Gasparrini, and F. Svelto, *Appl. Phys. Lett.* **17**, 105 (1978)
25. L. Mollard, G. Destefanis, N. Baier, J. Rothman, P. Ballet, J.P. Zanatta, et al., *J. Electron. Mater.* **38**, 1805 (2009)
26. N. Achtziger, J. Bollmann, Th. Licht, B. Reinhold, U. Reislöhner, J. Röhrich, M. Rüb, M. Wienecke, W. Witthuhn, *Semiconductor Science and Technology* **11**, 947 (1996)
27. M. Gettings, K.G. Stephens, *Radiat. Eff.* **22**, 53 (1974)
28. C. Uzan-Saguy, D. Comedi, V. Richter, R. Kalish, and R. Triboulet, *J. Vac. Sci. Technol. A* **7**, 2575 (1989)
29. P. Petrik, N.Q. Khanh, J. Li, J. Chen, R.W. Collins, M. Fried, et al., *Phys. Status Solidi Curr. Top. Solid State Phys.* **5**, 1358 (2008)
30. L.C. Feldman, J.W. Mayer, S.T. Picraux, *Materials Analysis by Ion Channeling*, (Academic Press 1982)
31. G. Leo, A. Traverse, M. O. Ruault, and A. V. Drigo, *Nucl. Instrum. Methods Phys. Res. B* **63**, 41 (1992)
32. G. Leo and M. O. Ruault, *J. Appl. Phys.* **73**, 2234 (1993)
33. G. Leo, A. V. Drigo, and A. Traverse, *Mater. Sci. Eng. B* **16**, 123 (1993)